

# Hydrothermal synthesis, crystal structure and magnetic property of a homodinuclear ternary coordination polymer of nickel(II)



Guo-Qing Zhong<sup>a,\*</sup>, Di Li<sup>a</sup>, Zhi-Peng Zhang<sup>b</sup>

<sup>a</sup> School of Material Science and Engineering, Southwest University of Science and Technology, Mianyang 621010, PR China

<sup>b</sup> Guilin Environmental Monitoring Centre, Guilin 541002, PR China

## ARTICLE INFO

### Article history:

Received 31 January 2016

Accepted 4 March 2016

Available online 17 March 2016

### Keywords:

Nickel(II) ternary complex

1,2,4,5-Benzenetetra-carboxylic acid

1,4-Bis(1H-imidazol-4-yl)benzene

Crystal structure

Magnetic measurement

## ABSTRACT

A novel transition metal–organic framework,  $[\text{Ni}_2(\mu_4\text{-btca})(1,4\text{-bib})_2(\text{H}_2\text{O})_2]_n$ , was obtained by the hydrothermal reaction of nickel chloride hexahydrate, 1,2,4,5-benzenetetra-carboxylic acid ( $\text{H}_4\text{btca}$ ) and 1,4-bis(1H-imidazol-4-yl)benzene (1,4-bib) in an ethanol aqueous solution. The composition and structure of the complex were characterized by elemental analyses, single crystal X-ray diffraction analysis, Fourier transform infrared spectroscopy, thermogravimetry and differential scanning calorimetry. The complex crystallizes in the triclinic system with the  $P\bar{1}$  space group. Each nickel(II) ion is hexacoordinated in a 2N4O mode and has a slightly distorted octahedral geometry. The thermal decomposition of the complex includes dehydration and pyrolysis of the ligands, and the final residue is nickel oxide. The magnetic property of the complex has been studied by variable temperature magnetic susceptibility measurements, and it possesses weak antiferromagnetic interactions.

© 2016 Elsevier Ltd. All rights reserved.

## 1. Introduction

The rational design and controlled synthesis of metal–organic frameworks (MOFs) and supramolecular coordination complexes, especially those constructed from predesigned bridging ligands and  $\pi$ – $\pi$  stacking interactions have attracted considerable attention and sustained growth due to their highly fascinating topological structures and potential applications, such as gas storage, magnetic materials, non-linear optics, ion exchange, chemical separation, catalytic agent and biomimetic chemistry, as well as being potential candidates for functional materials [1–9]. The shapes and the coordination behavior of the organic ligands are very important in the control of the frameworks [10]. It is well known that aromatic polycarboxylate ligands have various bridging ways and bent backbones, and can effectively link metal centers to generate MOFs, building self-penetrating, porous or helical coordination frameworks [11–15]. In fact, the diversity of coordination polymeric structures and their properties depend on many factors, such as ligand, solvent, pH value, metal ion, temperature, metal–ligand ratio, mixed-ligand and so forth [16,17]. Even small variations influence the synthetic process and change the framework structure [18–21].

Organic polycarboxylates are widely used as bridging ligands for designing polynuclear complexes, such as 1,2,4,5-benzenetetracarboxylic acid ( $\text{H}_4\text{btca}$ , or pyromellitic acid), which has four carboxyl groups and may be completely or only partially deprotonated, inducing a great many coordination modes [22–26]. Moreover, four carboxyl groups separated by a phenyl ring can form different dihedral angles through the rotation of C–C single bonds, leading to novel motifs with interesting magnetic properties. As a versatile ligand,  $\text{H}_4\text{btca}$  along with its versatile deprotonated forms have drawn considerable attention, especially in the preparation of novel high-dimensional functional coordination polymers [27–30]. Additionally, it can act as a hydrogen-bond acceptor and a hydrogen-bond donor, depending upon the degree of deprotonation, forming new extended structures by hydrogen bonding interactions [31,32]. However, it is important to select mixed bridging ligands; rigid bis(imidazole) based N-donor ligands are frequently used as ancillary ligands to give multipodal anions, acting as bridging [33]. Compared with bridging pyridyl ligands, 1,4-bis(1-imidazolyl)benzene possesses a favorable N-ligating donor set for metal ions. Various nickel pyromellitate complexes combined with N-donor aromatic ligands as a type of excellent rod-like connector to engender a wide range of coordination frameworks have been synthesized and structurally characterized, for instance  $[\text{Ni}(\text{btca})_{0.5}(\text{bimb})]_n$  [33] [bimb = 4,4'-bis(1-imidazolyl)biphenyl],  $[\text{Ni}_2(\text{btca})(\text{bpt})_2(\text{H}_2\text{O})_2] \cdot 6\text{H}_2\text{O}$  [34] [bpt = 1H-3,5-bis(4-pyridyl)-1,2,4-triazole],  $[\text{Ni}_2(\text{btca})(\text{bpy})_2(\text{H}_2\text{O})_2]_n \cdot 2n\text{H}_2\text{O}$  [35] (bpy = 4,4'-bipyridine),  $[\text{Ni}(\text{btca})_{0.5}(\text{Hbpt})(\text{H}_2\text{O})_3] \cdot 2\text{H}_2\text{O}$  [36]

\* Corresponding author. Tel.: +86 816 6089371; fax: +86 816 2419201.

E-mail address: [zqg316@163.com](mailto:zqg316@163.com) (G.-Q. Zhong).

[Hbpt = 1H-3-(3-pyridyl)-5-(4-pyridyl)-1,2,4-triazole],  $\{[\text{Ni}_2(\text{btca})(\text{bpym})(\text{H}_2\text{O})_4] \cdot 4\text{H}_2\text{O}\}_n$  [37] (bpym = 5,5'-bipyrimidine),  $\{[\text{Ni}_2(\text{btca})(\text{pyz})(\text{H}_2\text{O})_4] \cdot 2\text{H}_2\text{O}\}_n$  [38] (pyz = pyrazine),  $\text{Ni}_2(\text{btca})(\text{bpy})_3 \cdot 3\text{DMF}$  [39] (DMF = *N,N'*-dimethylformamide) and so on.

To our knowledge, nickel(II) is an essential ultra trace metal element for human nutrition, and it maintains normal physiological functions [40]. In this paper, 1,2,4,5-benzenetetracarboxylic acid is chosen as the primary anionic ligand, 1,4-bis(imidazol-1-yl)benzene (1,4-bib) acts as ancillary neutral ligand and nickel chloride hexahydrate acts as the central ion. We have synthesized a novel homodinuclear coordination polymer  $[\text{Ni}_2(\text{btca})(1,4\text{-bib})_2(\text{H}_2\text{O})_2]_n$  using the hydrothermal method. Herein, we report the composition and crystal structure of the complex, which has been characterized by elemental analyses, single crystal X-ray diffraction, FT-IR, TG-DSC and its magnetic property.

## 2. Experimental

### 2.1. Materials and physical measurements

The chemicals 1,2,4,5-benzenetetracarboxylic acid and 1,4-bis(1H-imidazol-4-yl)benzene were purchased from Jinan Henghua Sci. & Tec. Company Ltd., while nickel chloride hexahydrate was purchased from Merck Chemicals (Shanghai) Co., Ltd. All chemicals purchased were of analytical reagent grade and used without further purification.

The carbon, hydrogen and nitrogen contents in the complex were measured on a Perkin–Elmer 240 elemental analyzer and the nickel content was determined with a Thermo X-II inductively coupled plasma mass spectrometer. IR spectra were recorded from potassium bromide pellets in the range 4000–400  $\text{cm}^{-1}$  on a Perkin–Elmer Spectrum One spectrometer. Thermogravimetric analysis of the metal complex was performed by a SDT Q600 thermogravimetric analyzer, and the measurements were recorded from ambient temperature to 600 °C at a heating rate of 10 °C  $\text{min}^{-1}$  under an air flow of 100  $\text{mL min}^{-1}$ . The variable temperature magnetic susceptibility measurement of the complex was performed on a Quantum Design SQUID MPMS XL-7 instrument in the temperature range 2–300 K under a field of 1000 Oe.

### 2.2. Synthesis of the complex

A mixture of pyromellitic acid (0.15 mmol, 0.038 g), 1,4-bis(1H-imidazol-4-yl)benzene (0.30 mmol, 0.063 g), nickel chloride hexahydrate (0.30 mmol, 0.071 g), sodium hydroxide (0.40 mmol, 0.016 g), 2 mL ethanol, and 12 mL water was placed in a 30 mL Teflon-lined stainless steel vessel, heated at 170 °C for 72 h, followed by slow cooling to room temperature at a rate of 5 °C  $\text{h}^{-1}$ .

Green block crystals of the title complex were obtained. The crystals were collected by filtration, and dried at room temperature. The yield of the complex was 34% (based on Ni). *Anal. Calc.* for  $\text{Ni}_2\text{C}_{34}\text{H}_{26}\text{O}_{10}\text{N}_8$ : Ni, 14.24; C, 49.51; H, 3.16; N, 13.59. Found: Ni, 14.15; C, 49.21; H, 3.14; N, 13.51%.

### 2.3. X-ray crystallography

A single crystal of the title complex was studied on a Bruker Smart Apex II CCD diffractometer with graphite monochromated Mo K $\alpha$  radiation ( $\lambda = 0.71073$  Å) and  $\omega$ -2 $\theta$  scans. The data were collected at 298(2) K. A colorless and transparent crystal with dimensions 0.35 × 0.33 × 0.24 mm was mounted on a glass fibre. The structure was solved by direct methods with the SHELXS-97 program and refined on  $F^2$  by full-matrix least-squares using SHELXL-97 [41]. All non-hydrogen atoms were refined anisotropically. Hydrogen atoms of the organic ligands were placed at calculated positions and refined using the riding model. All water hydrogen atoms were found in difference Fourier maps and refined isotropically in the title complex.

## 3. Results and discussion

### 3.1. X-ray crystal structure analysis

The single crystal X-ray diffraction analysis revealed that the title complex crystallizes in the triclinic system with space group  $P\bar{1}$ . Crystallographic data and structure refinement parameters for the title complex are given in Table 1 and selected bond distances and angles are shown in Table S1. Key fragments of the structures and the atom numbering are shown in Fig. 1. The complex is the dinuclear species  $[\text{Ni}(1,4\text{-bib})(\text{H}_2\text{O})(\mu\text{-C}_6\text{H}_2(\text{COO})_4)\text{Ni}(1,4\text{-bib})(\text{H}_2\text{O})]$ . There are two crystallographically unique nickel(II) cations, one  $\text{btca}^{4-}$  anion ligand, two 1,4-bib neutral ligands and two coordinated water molecules in the asymmetrical structural unit. The pyromellitate ligands utilize the hydroxyl atoms O2 and O2#1 in the bridged coordination mode from the carboxylate group to link the nickel(II) cations, and the nuclear separation between the Ni1 and Ni1#1 atoms is 3.246 Å; this value is slightly larger than 3.079 Å from a dinuclear nickel(II) macrocyclic complex which is bis-bridged by phenolic oxygen atoms [42]. The two nickel(II) cations in the title complex show identical coordination environments, and the Ni1, O2, Ni1#1 and O2#1 atoms are in the same plane. The crystal packing diagram of the complex is shown in Fig. S1. Each nickel(II) center is hexacoordinated by two nitrogen atoms from two 1,4-bib ligands [ $\text{Ni1-N2} = 2.097(4)$  Å and  $\text{Ni1-N4} = 2.073(4)$  Å], three carboxyl oxygen atoms from two different  $\text{btca}^{4-}$  ligands [ $\text{Ni1-O3\#1} = 2.031(3)$  Å,  $\text{Ni1-O2\#1} = 2.066$

**Table 1**  
Crystal data and structure refinement parameters for the title complex.

Empirical formula	$\text{Ni}_2\text{C}_{34}\text{H}_{26}\text{O}_{10}\text{N}_8$	Absorption coefficient ( $\text{mm}^{-1}$ )	1.307
Formula weight ( $\text{g mol}^{-1}$ )	824.05	$F(000)$	422
$T$ (K)	293(2)	Crystal size ( $\text{mm}^3$ )	$0.35 \times 0.33 \times 0.24$
Wavelength (Å)	0.71073	Theta range for data collection (°)	2.61–25.02
Crystal system	triclinic	Limiting indices	$-9 \leq h \leq 7, -9 \leq k \leq 11, -11 \leq l \leq 11$
Space group	$P\bar{1}$	Reflections collected/unique	4427/2712 [ $R(\text{int}) = 0.0692$ ]
$a$ (Å)	8.0805(11)	Completeness to theta = 25.02	99.9%
$b$ (Å)	9.8771(12)	Absorption correction	Semi-empirical from equivalents
$c$ (Å)	10.0147(14)	Maximum and minimum transmission	0.7444 and 0.6576
$\alpha$ (°)	96.443(2)	Refinement method	Full-matrix least-squares on $F^2$
$\beta$ (°)	102.682(4)	Data/restraints/parameters	2712/0/244
$\gamma$ (°)	96.393(2)	Goodness-of-fit (GOF) on $F^2$	1.048
$V$ (Å <sup>3</sup> )	767.21(18)	Final $R$ indices [ $I > 2\sigma(I)$ ]	$R_1 = 0.0588, wR_2 = 0.1206$
$Z$	1	$R$ indices (all data)	$R_1 = 0.0806, wR_2 = 0.1396$
$D_{\text{calc}}$ ( $\text{g cm}^{-3}$ )	1.784	Largest difference peak and hole ( $\text{e Å}^{-3}$ )	0.614 and $-0.799$

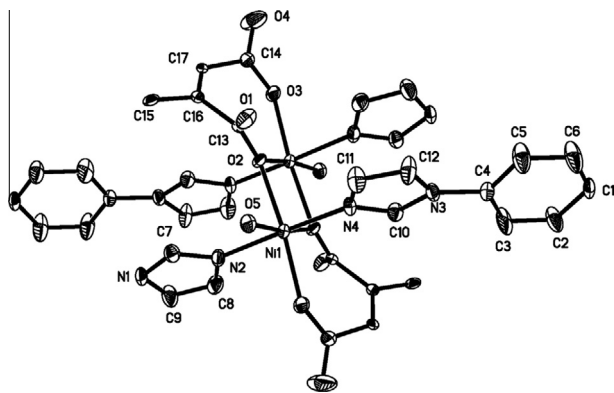


Fig. 1. The molecular structure of the title complex.

(3) Å and Ni1–O2 = 2.146(3) Å, and one oxygen atom [Ni1–O5 = 2.071(3) Å] from one water molecule, showing a slightly distorted octahedral coordination geometry with the four oxygen atoms in equatorial positions and two nitrogen atoms in axial positions [33], as shown in Fig. S2. Each pyromellitate linker is coordinated to four nickel centers in bidentate and monodentate fashions. The lengths of the Ni–O bonds and the Ni–N bonds are similar to those in Ref. [35], but the coordination structures of the title complex with the complex  $[\text{Co}_2(1,4\text{-bib})_2(\text{btca})]\cdot 2\text{H}_2\text{O}$  [17] are different. In this cobalt complex, containing the selfsame ligands, each Co(II) ion is tetrahedrally coordinated by two imidazole nitrogen atoms from two distinct 1,4-bib ligands, with Co–N bond lengths of 2.007(2) and 2.016(2) Å, and two monodentate carboxylate groups from two different  $\text{btca}^{4-}$  ligands, with Co–O bond lengths of 1.9713(18) and 1.986(2) Å. According to the C–O bond lengths [C13–O1 = 1.231(6) Å, C13–O2 = 1.273(6) Å, C14–O3 = 1.256(6) Å and C14–O4 = 1.215(6) Å], the three hydroxyl oxygen [O2, O3 and O2#1] atoms of the carboxylate groups from the  $\text{btca}^{4-}$  ligands are involved in coordination, and the carbonyl oxygen atoms of the carboxylate groups are not coordinated. In the dinuclear complex, the bond angles [O3#1–Ni1–O2#1 92.50°, O3#1–Ni1–O5 95.22°, O5–Ni1–O2 93.19° and O2#1–Ni1–O2 79.17°] add up to approximately 360° (360.08°); thus the Ni1, O3#1, O2#1, O2 and O5 atoms are nearly in the same plane. The  $\text{H}_4\text{btca}$  ligand in the title complex is completely deprotonated and bridges the metal nickel (II) ions through two carboxylate groups, forming a corrugated chain. The nickel(II) ions are also bridged by 1,4-bib ligands, resulting in a 1D fascinating ladder-like structure, which can be defined as a single left- or right-handed helix, as shown in Fig. 2. Finally, the ladders are extended to form a corrugated 2D network parallel to the  $bc$  crystal plane (Fig. 3). The pyromellitic acid is completely deprotonated and acts as one  $\mu_4$  node to coordinate with four nickel(II) ions, and the  $\text{btca}^{4-}$  ligands adopt  $\mu_4\text{-}\eta^1\eta^2\eta^1\eta^2$  coordination modes. The coordination modes of the four carboxylate groups in the  $\text{btca}^{4-}$  ligand can be divided into two kinds: two carboxylate groups of contra-position connect an adjacent nickel(II) ion with one O atom in a monodentate mode and elongate the structure into a 1D

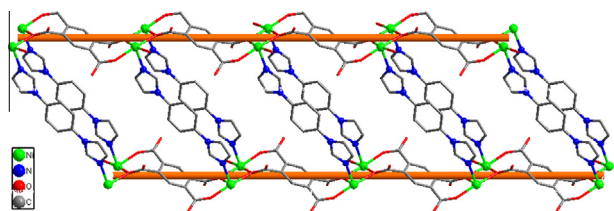


Fig. 2. 1D ladder chain formed by the  $\text{btca}^{4-}$  ligands connecting the nickel(II) ions.

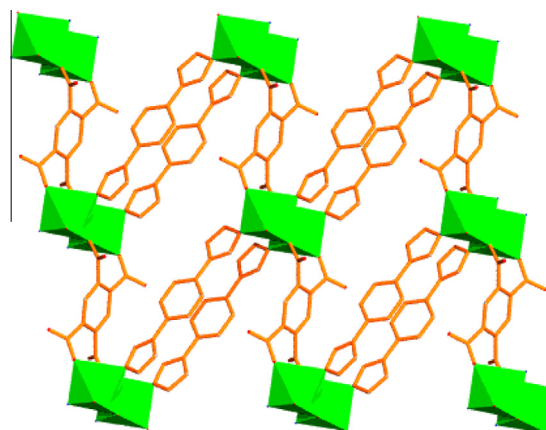


Fig. 3. View of the 3D framework with the 1,4-bib-bridged 2D nets.

chain along the  $b$  axis direction; the other two carboxylate groups of contra-position bond two adjacent nickel(II) ions with one O atom in a bidentate bridged mode, and the final the 2D layer structure is formed in the  $ab$  plane, stretching along the  $b$  axis direction.

As shown in Figs. 2 and 3, the molecules of the complex  $[\text{Ni}_2(\text{btca})(1,4\text{-bib})_2(\text{H}_2\text{O})_2]_n$  are held together by intermolecular hydrogen bonds. The hydrogen bond lengths and bond angles for the title complex are given in Table S2. A strong intramolecular hydrogen bond exists between the oxygen atom (O5) of the coordinated water molecules and the oxygen atom (O3) of a coordinated carboxylate group (O5–H5B...O3, 2.689 Å), and the oxygen atom (O5) forms the intermolecular hydrogen bonds O5–H5C...O1, 2.775 Å and O5–H5C...O4, 3.096 Å, respectively with the carboxylate O1 and O4 atoms. The distances between the imidazole rings situated in neighboring mirror planes are 3.423 and 3.659 Å (Fig. 4), which may indicate weak face-to-face  $\pi\text{-}\pi$  stacking interactions [28,43]. The existence of hydrogen bonds and  $\pi\text{-}\pi$  type interactions make the complex further connected, resulting in a three-dimensional framework structure.

### 3.2. FT-IR analysis

The FT-IR spectrum of the title complex is shown in Fig. S3. The infrared spectrum of the complex shows wide absorption bands in the region 3042–3400  $\text{cm}^{-1}$  can be assigned to the O–H stretching vibration of the water molecules, while a band at about 3146  $\text{cm}^{-1}$  suggests the O–H stretching vibration from the carboxyl group. Meanwhile, the coordinated water molecules exhibit the frequencies 650 and 584  $\text{cm}^{-1}$ , which are assigned to  $\rho_{\text{f}}(\text{H}_2\text{O})$  and  $\rho_{\text{w}}(\text{H}_2\text{O})$ . The absorption peak near 3042  $\text{cm}^{-1}$  is assigned to the C–H stretching vibration of the ligands. The absence of the band at ca. 1700  $\text{cm}^{-1}$  suggests the deprotonation of  $\text{H}_4\text{btca}$  in

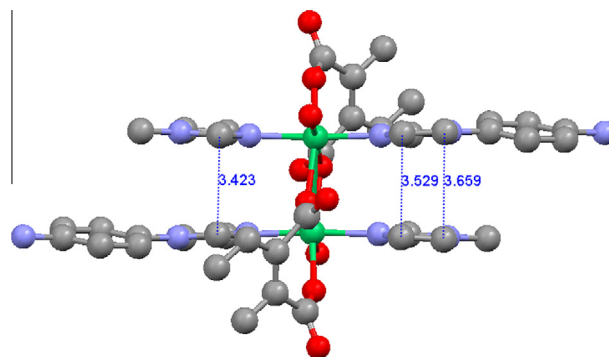


Fig. 4. Weak spatial  $\pi\text{-}\pi$  stacking interactions of the title complex.

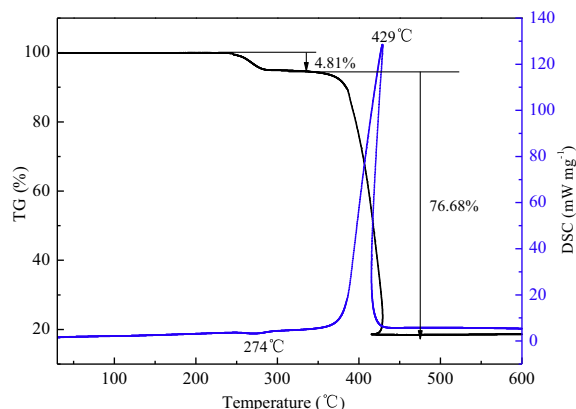


Fig. 5. TG-DSC curves of the title complex.

the complex. There are two symmetrical peaks at 1602, 1533 and 1353, 1310  $\text{cm}^{-1}$ , which are assigned to the  $\nu_{\text{as}}(\text{COO}^-)$  and  $\nu_{\text{s}}(\text{COO}^-)$  stretching vibrations, respectively. It confirms that the  $\text{btca}^{4-}$  ligand is coordinated to the nickel(II) ion. The difference in value of 180–292  $\text{cm}^{-1}$  between  $\nu_{\text{as}}(\text{COO}^-)$  and  $\nu_{\text{s}}(\text{COO}^-)$  is in line with a monodentate or bidentate bridge mode of the carboxylate group to the Ni(II) ion [44,45], which well agrees with corresponding result of the single crystal structure. In addition, characteristic absorption peaks at 1071, 832 and 717  $\text{cm}^{-1}$  can be assigned to the  $\nu(\text{C-N})$  stretching vibration of the 1,4-bib ligand [46]. In the far-infrared region, the absorption peak at 504  $\text{cm}^{-1}$  is assigned to the  $\nu(\text{Ni-N})$  stretching vibration and the absorption peaks at 464 and 422  $\text{cm}^{-1}$  are assigned to  $\nu(\text{Ni-O})$  stretching vibrations.

### 3.3. Thermal analysis

Studying the thermal decomposition process of complexes is helpful to understand the coordination structure of complexes [47,48]. The TG-DSC curves of the title complex are given in Fig. 5, and the possible pyrolysis reaction, the experimental and calculated percentage mass losses in the thermal decomposition process of the complex are summarized in Table S3. Fig. 5 shows that there is one weak endothermic peak and one strong exothermic peak in the DSC curve. The complex has good thermal stability before 230 °C. The first mass loss of the complex  $[\text{Ni}_2(\text{btca})(1,4\text{-}$

$\text{bib})_2(\text{H}_2\text{O})_2]_n$  occurs at about 274 °C in the DSC curve, corresponding to the release of two water molecules, then the complex becomes  $[\text{Ni}_2\text{C}_6\text{H}_2(\text{COO})_4(\text{C}_{12}\text{H}_{10}\text{N}_4)_2]$ . The experimental percentage mass loss (4.81%) is close to the calculated one (4.37%). The coordinated water molecules should be eliminated at higher temperatures than the water molecules of hydration. The water molecule of coordination is usually eliminated in the temperature range 100–316 °C [49,50]. Because of the high temperature for the loss of water, the two water molecules should be coordinated, which agrees well with the corresponding results of the single crystal structure and FT-IR spectra. The next step mass loss in the temperature range 350–450 °C corresponds to the total destruction of the framework by the oxidation of the organic component, and the experimental mass loss (76.68%) is close to the calculated one (77.50%). This is why there is an appreciable exothermic peak at 429 °C in the DSC curve. When the ligands are burnt completely, the residual mass of the complex remains almost constant in air until 500 °C, only the inorganic compound nickel oxide is obtained and the experimental result (18.51%) is in agreement with the result of the theoretical calculation (18.13%). The results of the thermal analysis further ascertain that the molecular composition of the complex is  $[\text{Ni}_2(\text{btca})(1,4\text{-bib})_2(\text{H}_2\text{O})_2]_n$ .

### 3.4. Magnetic property

The magnetic property of the title complex has been investigated by variable temperature magnetic susceptibility measurements in the solid state. The temperature dependence of  $\chi_{\text{m}}T$ ,  $1/\chi_{\text{m}}$  and  $\mu_{\text{eff}}$  for the title complex in the temperature range 2–300 K under a field of 1000 Oe is displayed in Fig. 6. The  $\chi_{\text{m}}T$  value of the nickel(II) complex at 300 K is 2.799  $\text{cm}^3 \text{K mol}^{-1}$ , which is larger than the expected value of 2  $\text{cm}^3 \text{K mol}^{-1}$  for two isolated nickel(II) ions [51]. The effective magnetic moment ( $\mu_{\text{eff}}$ ) value at room temperature is close to 4.731 B.M., using the equation  $\mu_{\text{eff}} = 2.828 \times (\chi_{\text{m}}T)^{1/2}$  [52]. This can be attributed to a contribution from the orbital angular momentum to the susceptibility at higher temperatures. While the temperature decreases, the  $\chi_{\text{m}}T$  values remain roughly constant down to 50 K and then  $\chi_{\text{m}}T$  increases rapidly and reaches a maximum of 5.564  $\text{cm}^3 \text{K mol}^{-1}$  at 2 K. The gradual increase of  $\mu_{\text{eff}}$  upon cooling suggests the presence of weak antiferromagnetic spin-exchange interactions between the two nickel(II) ions within each molecule. The plot of  $\chi_{\text{m}}^{-1}$  versus  $T$  over the temperature range 20–300 K agrees with the Curie-Weiss law [ $\chi_{\text{m}} = C/(T - \theta)$ ], with  $C = 2.92 \text{ cm}^3 \text{K mol}^{-1}$

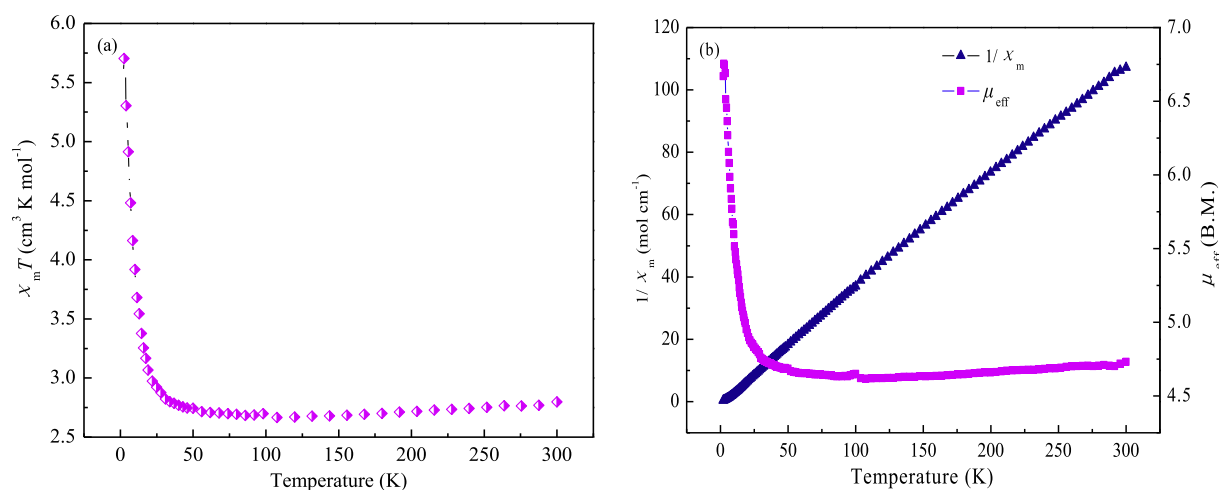


Fig. 6. Temperature dependence of  $\chi_{\text{m}}T$  (a),  $1/\chi_{\text{m}}$  and  $\mu_{\text{eff}}$  (b) for the title complex.

and  $\theta = -8.2$  K. The negative Weiss constant conclusively evidences the presence antiferromagnetic interactions between the nickel(II) ions in the complex. In addition, the magnetic properties of a series of oxygen bridged dinuclear compounds show that when the included angle between Ni–O–Ni is less than  $97^\circ$ , a ferromagnetic interaction is present between the Ni(II)–Ni(II) unit; when the included angle between Ni–O–Ni is higher than  $97^\circ$ , there an anti-ferromagnetic interaction between the Ni(II)–Ni(II) unit [53]. In the title complex, the Ni(1)–O(2)–Ni(1) bond angle is  $100.83^\circ$ ; this further proves that the complex should exhibit an antiferromagnetic interaction. The fitting result is comparable with those reported for other coupled nickel(II) dimers.

#### 4. Conclusions

The homodinuclear ternary coordination polymer  $[\text{Ni}_2(\mu_2\text{-btca})(1,4\text{-bib})_2(\text{H}_2\text{O})_2]_n$  was synthesized with nickel chloride, 1,2,4,5-benzenetetracarboxylic acid and 1,4-bis(1H-imidazol-4-yl)benzene as the reactants by a hydrothermal method in an ethanol aqueous solution. The composition and structure of the complex were characterized by EA, FTIR, single crystal X-ray diffraction and TG-DSC. The crystal structure of the nickel(II) complex belongs to the triclinic system, space group  $P\bar{1}$ , with cell parameters  $a = 8.0805(11)$  Å,  $b = 9.8771(12)$  Å,  $c = 10.0147(14)$  Å,  $\alpha = 96.443(2)^\circ$ ,  $\beta = 102.682(4)^\circ$  and  $\gamma = 96.393(2)^\circ$ . In this complex, the carboxylate group of the pyromellitic acid acts as a bridge between the nickel(II) ions, and the two nickel(II) ions are both hexacoordinated by two nitrogen atoms from two imidazole rings, three carboxyl oxygen atoms from different btca<sup>4-</sup> ligands and one oxygen atom from a coordinated water molecule, with a slightly distorted octahedral geometry. The thermal decomposition processes of the complex under air include dehydration and pyrolysis of the ligands, and the final residue at about  $450^\circ\text{C}$  is nickel oxide. The complex possesses weak antiferromagnetic interactions between the two Ni(II) metal centers.

#### Acknowledgements

This work was supported by the National Natural Science Foundation of China (No. 21201142) and the Scientific Research Funds of Department of Education of Sichuan Province, PR China (No. 10ZA016).

#### Appendix A. Supplementary data

CCDC 989287 contains the supplementary crystallographic data for complex  $[\text{Ni}_2(\mu_4\text{-btca})(1,4\text{-bib})_2(\text{H}_2\text{O})_2]_n$ . These data can be obtained free of charge via <http://www.ccdc.cam.ac.uk/conts/retrieving.html>, or from the Cambridge Crystallographic Data Centre, 12 Union Road, Cambridge CB2 1EZ, UK; fax: (+44) 1223-336-033; or e-mail: [deposit@ccdc.cam.ac.uk](mailto:deposit@ccdc.cam.ac.uk). Supplementary data associated with this article can be found, in the online version, at <http://dx.doi.org/10.1016/j.poly.2016.03.020>.

#### References

- [1] M. Wriedt, A.A. Yakovenko, G.J. Halder, A.V. Prosvirin, K.R. Dunbar, H.C. Zhou, *J. Am. Chem. Soc.* 135 (2013) 4040.
- [2] J. Cui, Y. Li, Z. Guo, H. Zheng, *Chem. Commun.* 49 (2013) 555.
- [3] L. Fan, X. Zhang, Z. Sun, W. Zhang, Y. Ding, W. Fan, H. Lei, *Cryst. Growth Des.* 13 (2013) 2462.
- [4] N. Saravanan, M. Sankaralingam, M. Palaniandavar, *RSC Adv.* 4 (2014) 12000.

- [5] W.Q. Kan, S.Z. Wen, Y.H. Kan, H.Y. Hu, S.Y. Niu, X.Y. Zhang, *Polyhedron* 85 (2015) 246.
- [6] X.T. Zhang, L.M. Fan, Z. Sun, W. Zhang, D.C. Li, J.M. Dou, L. Han, *Cryst. Growth Des.* 13 (2013) 792.
- [7] X.T. Zhang, D. Sun, B. Li, L.M. Fan, B. Li, H. Wei, *Cryst. Growth Des.* 12 (2012) 3845.
- [8] S. Su, Y. Zhang, M. Zhu, X. Song, S. Wang, S. Zhao, H. Zhang, *Chem. Commun.* 48 (2012) 11118.
- [9] G.X. Liu, H. Xu, X.M. Ren, *Chin. J. Struct. Chem.* 29 (2010) 1792.
- [10] L.M. Zhao, B. Zhai, D.L. Gao, W. Shi, B. Zhao, P. Cheng, *Inorg. Chem. Commun.* 13 (2010) 1014.
- [11] P. Silva, L. Cunha-Silva, N.J.O. Silva, J. Rocha, F.A.A. Paz, *Cryst. Growth Des.* 13 (2013) 2607.
- [12] X.T. Zhang, L.M. Fan, X. Zhao, D. Sun, D.C. Li, J.M. Dou, *CrystEngComm* 14 (2012) 2053.
- [13] J.H. He, D.Z. Sun, D.R. Xiao, S.W. Yan, H.Y. Chen, X. Wang, J. Yang, E.B. Wang, *Polyhedron* 42 (2012) 24.
- [14] J.M. Lim, P. Kim, M.C. Yoon, J. Sung, V. Dehm, Z.J. Chen, F. Wurthner, D. Kim, *Chem. Sci.* 4 (2013) 388.
- [15] E.C. Yang, X.Y. Zhang, X.G. Wang, Z.Y. Liu, X.J. Zhao, *Polyhedron* 53 (2013) 208.
- [16] H. Wu, H.Y. Liu, J. Yang, B. Liu, J.F. Ma, Y.Y. Liu, Y.Y. Liu, *Cryst. Growth Des.* 11 (2011) 2317.
- [17] S.S. Chen, Y. Zhao, J. Fan, T. Okamura, Z.S. Bai, Z.H. Chen, W.Y. Sun, *CrystEngComm* 14 (2012) 3564.
- [18] F. Costantino, A. Ienco, S. Midollini, *Cryst. Growth Des.* 10 (2009) 7.
- [19] A.C. Tsiapis, *RSC Adv.* 4 (2014) 32504.
- [20] L. Cañadillas-Delgado, J. Pasán, O. Fabelo, M. Julve, F. Lloret, C. Ruiz-Pérez, *Polyhedron* 52 (2013) 321.
- [21] A.D. Burrows, *CrystEngComm* 13 (2011) 3623.
- [22] Q. Shi, R. Cao, D.F. Sun, M.C. Hong, Y.C. Liang, *Polyhedron* 20 (2001) 3287.
- [23] H. Kumagai, K.W. Chapman, C.J. Kepert, M. Kurmoo, *Polyhedron* 22 (2003) 1921.
- [24] S. Konar, P.S. Mukherjee, M.G. Drew, J. Ribas, N.R. Chaudhuri, *Inorg. Chem.* 42 (2003) 2545.
- [25] L.J. Zhang, J.Q. Xu, Z. Shi, X.L. Zhao, T.G. Wang, *J. Solid State Chem.* 173 (2003) 32.
- [26] C.C. Correa, R. Diniz, J. Janczak, M.I. Yoshida, L.F.C. de Oliveira, F.C. Machado, *Polyhedron* 29 (2010) 3125.
- [27] H.K. Zhao, B. Ding, E.C. Yang, X.G. Wang, X.J. Zhao, *Z. Anorg. Allg. Chem.* 633 (2007) 1735.
- [28] R.P. Liu, X.W. Yang, L.J. Wang, F. Liu, L.L. Zhang, F.S. Yu, S.P. Chen, *Chin. J. Chem.* 27 (2009) 1827.
- [29] L.P. Sun, S.Y. Niu, J. Jin, G.D. Yang, L. Ye, *Eur. J. Inorg. Chem.* (2006) 5130.
- [30] Y. Feng, E.C. Yang, M. Fu, X.J. Zhao, *Z. Anorg. Allg. Chem.* 636 (2010) 253.
- [31] D. Wilms, F. Wurm, J. Nieberle, P. Böhm, U. Kemmer-Jonas, H. Frey, *Macromolecules* 42 (2009) 3230.
- [32] D. Tian, Y. Pang, Y.H. Zhou, L. Guan, H. Zhang, *CrystEngComm* 13 (2011) 957.
- [33] L.L. Wen, J.B. Zhao, K.L. Lv, Y.H. Wu, K.J. Deng, X.K. Leng, D.F. Li, *Cryst. Growth Des.* 12 (2012) 1603.
- [34] F.P. Huang, H.Y. Li, Q. Yu, H.D. Bian, J.L. Tian, S.P. Yan, D.Z. Liao, P. Cheng, *CrystEngComm* 14 (2012) 4756.
- [35] C.D. Wu, C.Z. Lu, S.F. Lu, H.H. Zhuang, J.S. Huang, *Inorg. Chem. Commun.* 5 (2002) 171.
- [36] B. Li, S.P. Chen, Q. Yang, S.L. Gao, *Polyhedron* 30 (2011) 1213.
- [37] T.W. Tseng, T.T. Luo, C.C. Tsai, J.Y. Wu, H.L. Tsai, K.L. Lu, *Eur. J. Inorg. Chem.* (2010) 3750.
- [38] S.Y. Yang, L.S. Long, R.B. Huang, L.S. Zheng, S.W. Ng, *Acta Cryst.* E59 (2003) m734.
- [39] C.Y. Gao, S.X. Liu, L.H. Xie, C.Y. Sun, J.F. Cao, Y.H. Ren, D. Feng, Z.M. Su, *CrystEngComm* 11 (2009) 177.
- [40] U.C. Gupta, S.C. Gupta, *Commun. Soil Sci. Plan.* 29 (1998) 1491.
- [41] G.M. Sheldrick, *Acta Cryst.* A64 (2008) 112.
- [42] Y.Y. Jiang, J.F. Ma, Y.Y. Liu, J. Yang, *J. Chem. Crystallogr.* 41 (2011) 286.
- [43] S. Sando, S. Goswami, H.S. Jena, S. Parshamoni, S. Konar, *CrystEngComm* 16 (2014) 4742.
- [44] G.Q. Zhong, J. Shen, Q.Y. Jiang, K.B. Yu, *Chin. J. Chem.* 29 (2011) 2650.
- [45] Q. Zang, G.Q. Zhong, M.L. Wang, *Polyhedron* 100 (2015) 223.
- [46] G.Q. Zhong, Y. Zhang, *Asian J. Chem.* 25 (2013) 9551.
- [47] N. Zhao, S.P. Wang, R.X. Ma, Z.H. Gao, R.F. Wang, J.J. Zhang, *J. Alloys Compd.* 463 (2008) 338.
- [48] G.Q. Zhong, J. Shen, Q.Y. Jiang, Y.Q. Jia, M.J. Chen, Z.P. Zhang, *J. Therm. Anal. Calorim.* 92 (2008) 607.
- [49] G.Q. Zhong, Q. Zhong, *Green Chem. Lett. Rev.* 7 (2014) 236.
- [50] W. Zhang, W. He, X.R. Guo, Y.W. Chen, L.M. Wu, D.C. Guo, *J. Alloys Compd.* 620 (2015) 383.
- [51] X.H. Zhou, *Chin. J. Inorg. Chem.* 26 (2010) 801.
- [52] H.L. Jia, L.F. Hou, Y. Zhang, P.F. Yuan, G. Li, *Chin. J. Inorg. Chem.* 29 (2013) 1897.
- [53] A. Karmakar, R.J. Sarma, J.B. Baruah, *Eur. J. Inorg. Chem.* 2006 (2006) 4673.